SMC-TR-06-10

AEROSPACE REPORT NO.
TR-2006(8570)-3

Radial Diffusion as a Potential Source and Loss Mechanism of Relativistic Electrons in the Outer Radiation Belt

15 February 2006

Prepared by

Y. Y. SHPRITS,[1,2] R. M. THORNE,[1] R. FRIEDEL,[2]
G. D. REEVES,[2] J. FENNELL,[3] D. N. BAKER,[4]
and S. G. KANEKAL[4]

[1]University of California, Los Angeles
[2]Los Alamos National Laboratory, Los Alamos, NM
[3]The Aerospace Corporation, El Segundo, CA
[4]Laboratory for Atmospheric and Space Physics, Boulder, CO

Prepared for

SPACE AND MISSILE SYSTEMS CENTER
AIR FORCE SPACE COMMAND
483 N. Aviation Blvd.
El Segundo, CA 90245-2808

Engineering and Technology Group

THE AEROSPACE CORPORATION
El Segundo, California

This report was submitted by The Aerospace Corporation, El Segundo, CA 90245-4691, under Contract No. FA8802-04-C-0001 with the Space and Missile Systems Center, 483 N. Aviation Blvd., El Segundo, CA 90245. It was reviewed and approved for The Aerospace Corporation by J. A. Hackwell, Principal Director, Space Science Applications Laboratory; and D. C. Marvin, Principal Director, Office of Research & Technology Applications. Michael Zambrana was the project officer for the Mission-Oriented Investigation and Experimentation (MOIE) program.

This report has been reviewed by the Public Affairs Office (PAS) and is releasable to the National Technical Information Service (NTIS). At NTIS, it will be available to the general public, including foreign nationals.

This technical report has been reviewed and is approved for publication. Publication of this report does not constitute Air Force approval of the report's findings or conclusions. It is published only for the exchange and stimulation of ideas.

Michael Zambrana
SMC/EA

REPORT DOCUMENTATION PAGE

Form Approved
OMB No. 0704-0188

1. REPORT DATE (*DD-MM-YYYY*)	2. REPORT TYPE	3. DATES COVERED *(From - To)*
15-02-2006		

4. TITLE AND SUBTITLE

Radial Diffusion as a Potential Source and Loss Mechanism of Relativistic Electrons in the Outer Radiation Belt

5a. CONTRACT NUMBER
FA8802-04-C-0001

5b. GRANT NUMBER

5c. PROGRAM ELEMENT NUMBER

6. AUTHOR(S)

Y. Y. Shprits, R. M. Thorne, R. Friedel, G. D. Reeves, J. Fennell, D. N. Baker, and S. G. Kanekal

5d. PROJECT NUMBER

5e. TASK NUMBER

5f. WORK UNIT NUMBER

7. PERFORMING ORGANIZATION NAME(S) AND ADDRESS(ES)

The Aerospace Corporation
Laboratory Operations
El Segundo, CA 90245-4691

8. PERFORMING ORGANIZATION REPORT NUMBER

TR-2006(8570)-3

9. SPONSORING / MONITORING AGENCY NAME(S) AND ADDRESS(ES)

Space and Missile Systems Center
Air Force Space Command
483 N. Aviation Blvd.
El Segundo, CA 90245

10. SPONSOR/MONITOR'S ACRONYM(S)
SMC

11. SPONSOR/MONITOR'S REPORT NUMBER(S)
SMC-TR-06-10

12. DISTRIBUTION/AVAILABILITY STATEMENT

Approved for public release; distribution unlimited.

13. SUPPLEMENTARY NOTES

14. ABSTRACT

The loss mechanisms responsible for the sudden depletions of the outer electron radiation belt are examined based on observations and radial diffusion modeling. SAMPEX data for Oct–Dec 2003, indicates that depletions are correlated with increases in geomagnetic activity and are also correlated with sudden increases in the solar wind dynamic pressure. Multi-channel HEO observations show that depletions at higher L are seen at energies as low as a few hundred keV. For the same events, high-energy proton channels also show decrease in fluxes at higher L-values. These observations are consistent with outward radial diffusion driven by the loss to magnetopause at $L > 4$. We further examine the viability of the outward radial diffusion loss by comparing CRRES observations with a radial diffusion model simulation. Model-data comparison shows that flux variation near geosynchronous orbit can be effectively propagated by the outward radial diffusion to $L = 4$ and can account for the main phase storm depletions.

15. SUBJECT TERMS

Radiation belts, Relativistic electrons, Radial diffusion

16. SECURITY CLASSIFICATION OF:			17. LIMITATION OF ABSTRACT	18. NUMBER OF PAGES	19a. NAME OF RESPONSIBLE PERSON
					Joseph Fennell
a. REPORT	b. ABSTRACT	c. THIS PAGE			19b. TELEPHONE NUMBER *(include area code)*
UNCLASSIFIED	UNCLASSIFIED	UNCLASSIFIED		21	(310)336-7075

Acknowledgements

This research was supported in part by IGPP LANL Collaborative Research mini-grant and NASA grants NNG04GN44G and NAG5-11324. The work at The Aerospace Corporation was supported by a NASA LWS DATM grant NAG5-10972 and The Aerospace Corporation MOIE program (via U. S. Air Force under Contract No. FA8802-04-C-0001).

Contents

Figures

1. Introduction

The electron radiation belts exhibit a two-zone structure. The inner radiation belt is very stable, while the outer belt shows high variability in the magnitudes of electron fluxes, the location of the peak of fluxes, and the duration of the intervals of depleted and enhanced electron fluxes. During geomagnetically quiet times, a "slot" region, separating the inner and the outer radiation belts, is formed as a result of the inward radial diffusion and losses to the atmosphere [*Lyons and Thorne, 1973*]. During disturbed geomagnetic conditions, the slot region is occasionally refilled [*Thorne and Russell, 1971*], and the plasmapause can be compressed down to low L values [*Baker et al., 2005*], which creates preferential conditions for the local acceleration (low plasma density and strong magnetic field) [*Horne et al., 2005*].

O'Brien et al., [2001] showed that increases in relativistic electron fluxes at geosynchronous orbit are correlated with the ULF wave activity, which is consistent with a radial diffusion acceleration mechanism. However, radial diffusion model simulations are incapable of reproducing the build up of peaks in phase space density [*Brautigam and Albert, 2000 and Shprits and Thorne, 2004*], frequently observed in the recovery phase of the storms [*Green and Kivelson, 2004*]. *Shprits et al.* [2005a] performed the radial diffusion simulations with constant outer boundary conditions and a variable lifetime parameter and concluded that both acceleration mechanisms occur on similar time scales and that both mechanisms contribute to the variability of the relativistic electron fluxes in the radiation belts.

Flux variations can generally be divided into two categories: adiabatic or reversible changes, and non-adiabatic or irreversible. Adiabatic changes in electron fluxes occur when the magnetic field changes slowly compared to the timescale associated with the particle adiabatic invariants [*Roederer, 1970*]. When the magnetic field slowly decreases due to an increase in the storm-time ring current, electrons move out to conserve the third invariant, and will loose energy to conserve the first adiabatic invariant. When either the gradient of the energy spectrum or the radial gradient is steep, the radial displacement of electrons will result in significant changes of electron fluxes at a fixed radial distance and energy as observed by spacecraft [*Li et al., 1997; Kim and Chan 1997; Reeves et al., 1998*]. To explain the net effect of adiabatic variations, it is instructive to consider two extreme cases when particles move outward due to decreases in magnetic field. If there is no radial gradient in PSD, but there is a declining spectrum, the spacecraft will see fewer particles at a fixed energy because they originate from an initial (smaller) population at higher energies. On the other hand, if the energy spectrum is flat but there is an inward radial gradient (more particles at lower L-values), the spacecraft will measure an increase in electron fluxes. The magnitude of the adiabatic flux variations will depend on the steepness of the energy spectrum, radial gradients, the magnitude of the disturbance in the field, and the background magnetic field. The strongest effect is usually at higher L shells where the background magnetic field tends to be weaker [*Kim and Chan, 1997*]. For many storms, fluxes do not return to the original pre-storm values, which indicates that non-adiabatic losses occur during storms [*McAdams and Reeves, 2001; Onsager et al., 2002, Green et al., 2004*]. The net effect of

losses during storms could be compensated by the various enhanced sources of electrons [Reeves et al., 2003].

Significant progress has been made in recent years in quantifying non-adiabatic loss mechanisms in the radiation belts. Losses inside the plasmasphere are predominantly due to whistler mode hiss wave scattering with loss timescales on the order of 5 to 10 days [*Lyons et al., 1972; Albert, 1994; Abel and Thorne, 1998*]. *Meredith et al.* [2004] also demonstrated that the intensity of the hiss, and consequently the rate of pitch angle scattering, are correlated with the level of geomagnetic activity.

From radial diffusion simulations, *Shprits et al.*, [2005a] concluded that effective losses in the heart of the radiation belts (where the outer radiation belt fluxes maximize) usually occur on the timescale of a day, which is much shorter than timescales associated with plasmaspheric hiss. This conclusion is supported by the theoretical estimates of the scattering rates due to chorus waves, which indicate that such losses occur throughout the outer radiation belt [*Albert, 2005; Horne et al., 2005; Thorne et al., 2005b*]. Combined SAMPEX and Polar observations also show that microburst precipitation, which is thought to be produced by bursty chorus waves, can provide electron losses on the scale of a day or less throughout the outer radiation belt zone [*O'Brien et al., 2004; Thorne et al., 2005b*].

EMIC waves could provide fast, localized losses on the time scale of hours [*Thorne and Kennel, 1971; Albert 2003; Summers and Thorne, 2003*]. These waves are preferentially excited in the high-density plasmasphere, along the dusk side plasmapause [*Horne and Thorne, 1993; Kozyra et al., 1997; Jordanova et al., 2001a,b*], during enhanced convective injection of the ring current ions. In the vicinity of the plasmapause, the minimum electron energy for resonance can drop to 500 keV [*Meredith et al., 2003; Summers and Thorne, 2003*]. Resonant relativistic electrons only briefly traverse the dusk side region of intense EMIC waves, but may produce very rapid precipitation events that are strongly localized in MLT. Precipitation due to EMIC waves may be also related to the bursts of hard X-rays seen by balloon-born instruments [*Millan et al 2002*].

Even though radial diffusion rates are strongest during the main phase of the storm and are capable of effectively transporting electrons to lower L shells and accelerating them, electron fluxes are commonly observed to decrease during the main phase of a storm [*e.g., Nagai, 1988, Mathie and Mann, 2000; O'Brien et al., 2001, Onsager, 2002*].

Green et al. [2004] concluded that such losses can not be produced by magnetopause encounters alone since losses extended much further into the heart of the radiation belts than the estimated stormtime magnetopause location. In this study, we attempt to verify whether inward gradients in phase space density created by the losses to magnetopause and consequent outward radial diffusion that acts to minimize these gradients are capable of contributing to the main phase depletions of the radiation belts, and thus produce flux drop outs at lower L-values.

In Section 2, we present SAMPEX observations of a 70-day period in October, November, and December 2003. We show that the flux drop outs are not adiabatic, are well correlated with increases in Kp, and are also correlated with increases in the solar wind dynamic pressure. To determine whether the main phase drop outs are a result of scattering by EMIC waves or outward radial diffusion, we present multi-energy HEO observations in Section 3 as well as HEO proton measurements.

To verify the viability and efficiency of the outward radial diffusion loss, in Section 4, 5, and 6, we present radial diffusion simulations with the variable outer boundary and show how electron flux variations near geosynchronous orbit affect fluxes at lower L-shells by means of outward or inward radial diffusion.

2. SAMPEX Observations

Figure 1 shows the evolution of the 2–6 MeV electron fluxes observed by the PET instrument on SAMPEX starting on DOY 290, 2003 (October 17) for 70 days. The variability of the electron fluxes and formation of the new radiation belt during these strong geomagnetic storms have been previously reported and studied by *Baker et al. [2004], Horne et al. [2005], Shprits et al. [2005b], Thorne et al. [2005a]*. Clearly evident are the formation of new radiation belts in the slot region in the recovery phases of the October 31 and November 20 storms (DOY 304 and 324). Also evident are increases in the inner radiation belt ($L < 2$) following the rapid refilling of the slot region. In this study, we concentrate on depletions of the radiation belts during this time period. Part of the drop out in fluxes may be associated with adiabatic changes. For most of the storms shown on Figure 1, *Dst* recovers before the fluxes come back to pre-storm values, which indicates that non-adiabatic losses occur during the main phases of the storms.

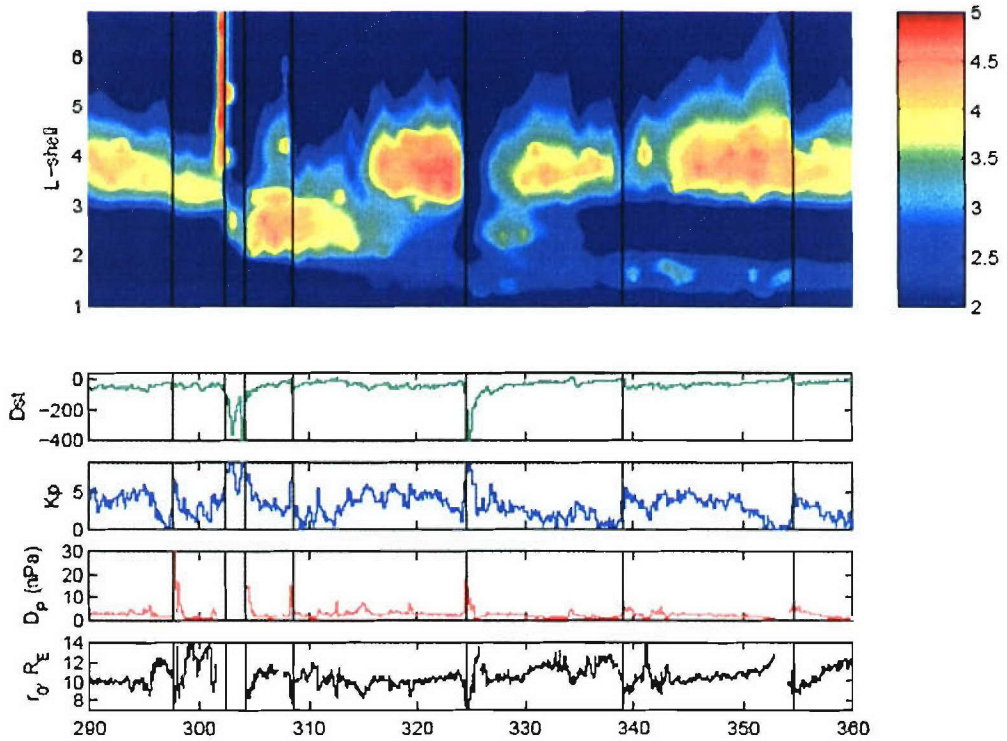

Figure 1. SAMPEX observations of 2–6 MeV electron fluxes in $\log_{10}(cm^{-2}\ sr^{-1}\ s^{-1})$ from October 17 till December 26, 2003 (top panel). Evolution of the *Dst* index (second panel), *Kp* (third panel), and solar wind dynamic pressure inferred from ACE measurements in $km^2\ s^1\ cc^1$ (fourth panel) and estimated Magnetopause location (bottom panel).

If the inward radial diffusion was the only acceleration mechanism, and it operated throughout the outer radiation zone, the increases in ULF wave activity and increases in *Kp* should correspond to flux increases. In contrast, Figure 1 shows that each of the depletions (October 24,29, 31, November 4, 20, December 4, 20, which correspond to DOY 297, 302, 304, 308, 324, 338, 354) occurred when the *Kp* index suddenly increased. Such catastrophic decreases in fluxes during disturbed geomagnetic conditions could be explained either by increased EMIC wave activity and pitch angle scattering into a loss cone [*Summers and Thorne, 2003; Albert, 2003*], or it could be due to the outward radial diffusion driven by losses to the magnetopause. As shown on the forth panel of Figure 1, the solar wind dynamic pressure (*Dp*) increases for each of these events, causes a compression of magnetopause, and consequently losses on the dayside. The bottom panel of Figure 1 shows the magnetopause standoff distance, estimated using the *Shue et al., [1997]* model, which moves inward in response to the increases in the solar wind dynamic pressure. Some of the magnetopause compressions, such as on November 8 (DOY 312), do not produce a significant drop in *Dst*, but clearly produce depletions in the outer radiation belt zone, which again indicates that losses associated with increases in *Kp* and solar wind dynamic pressure are irreversible.

3. HEO Multi-Channel Observations

Since EMIC waves only interact with electrons at energies ≥0.5 MeV [*Meredith et al., 2004, Summers and Thorne, 2003*], precipitation loss from EMIC scattering can be separated from losses due to the outward radial diffusion by comparing the evolution of fluxes at various energies. Figure 2 shows Highly Elliptical Orbit (HEO) satellite observations at six energy channels ranging from $E >$ 0.13 MeV to $E > 3$ MeV. The depletions of relativistic electrons are seen simultaneously on the low-orbiting SAMPEX and the polar-orbiting HEO spacecrafts. The comparison of SAMPEX and HEO observations suggests that electron flux drop outs occur over a broad range of pitch angles and at all local times. For the same events, as described in Section 2, HEO observations show that all channels (including $E > 0.13$ and $E > 0.23$ MeV) are depleted down to $L = 4$ during the main phases of the strong storms. Such loss can not be explained by the EMIC wave scattering. However, EMIC waves may contribute to depletions at lower L-values.

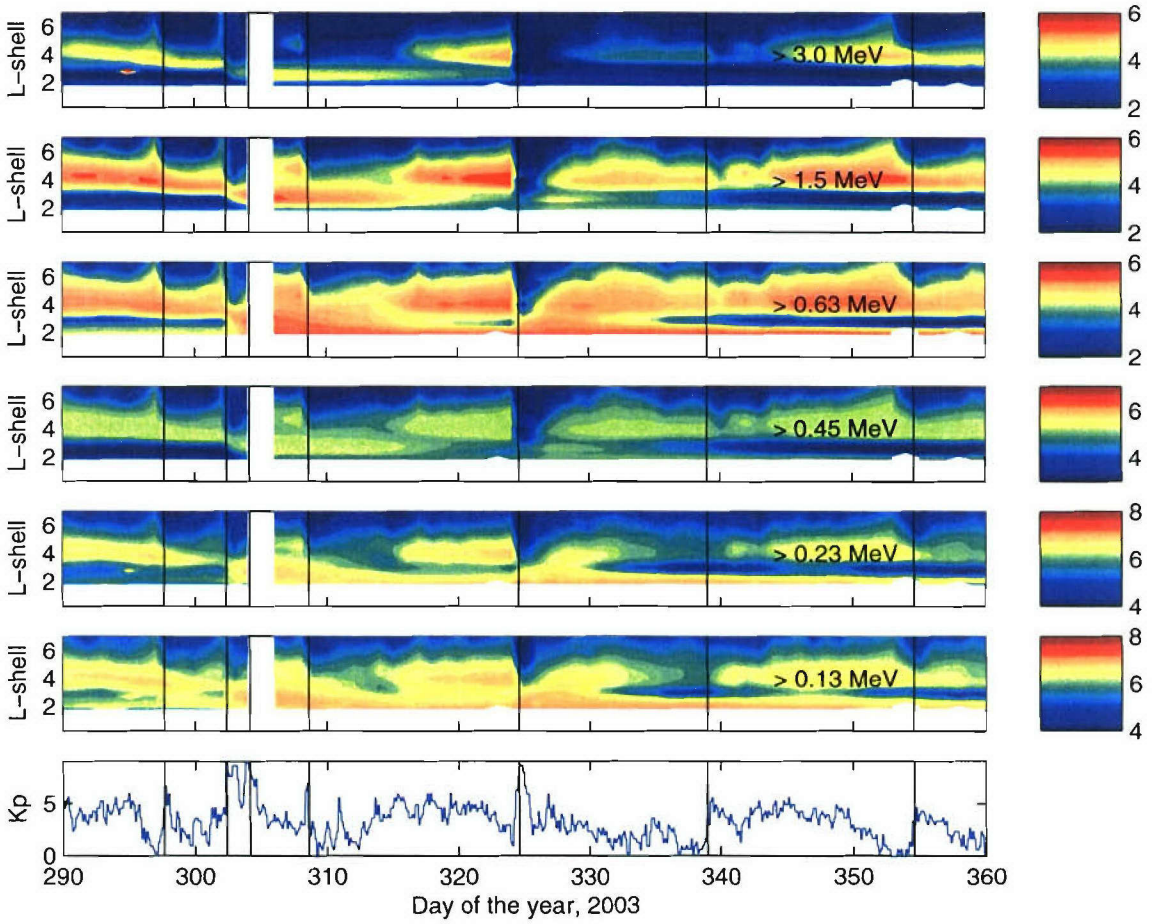

Figure 2. Integrated electron flux measured on HEO for energies > 3.0, 1.5 0.63, 0.45, 0.23, and 0.13 MeV (first 6 panels) in $\log_{10}(\text{cm}^{-2}\ \text{sr}^{-1}\ \text{s}^{-1})$ and the *Kp* index (bottom).

Any loss to the magnetopause, driven by outward radial diffusion, should affect both electrons and protons. Some of the HEO proton channels are affected by energetic electrons and are not suitable for comparison to electron and proton fluxes. Figure 3 shows a comparison between the > 1.5 .MeV electron channel and >320 keV proton channel. Note that the new electron radiation belt, formed on DOYs 302–318 between $L = 2$ and 4 [*Baker et al., 2004*], is not apparent on this proton channel, indicating little contamination from the high-energy electrons. During the strongest electron drop out events, proton fluxes also show depletions. The most dramatic loss of relativistic electrons and protons is seen during the November 20 storm (DOY 324).

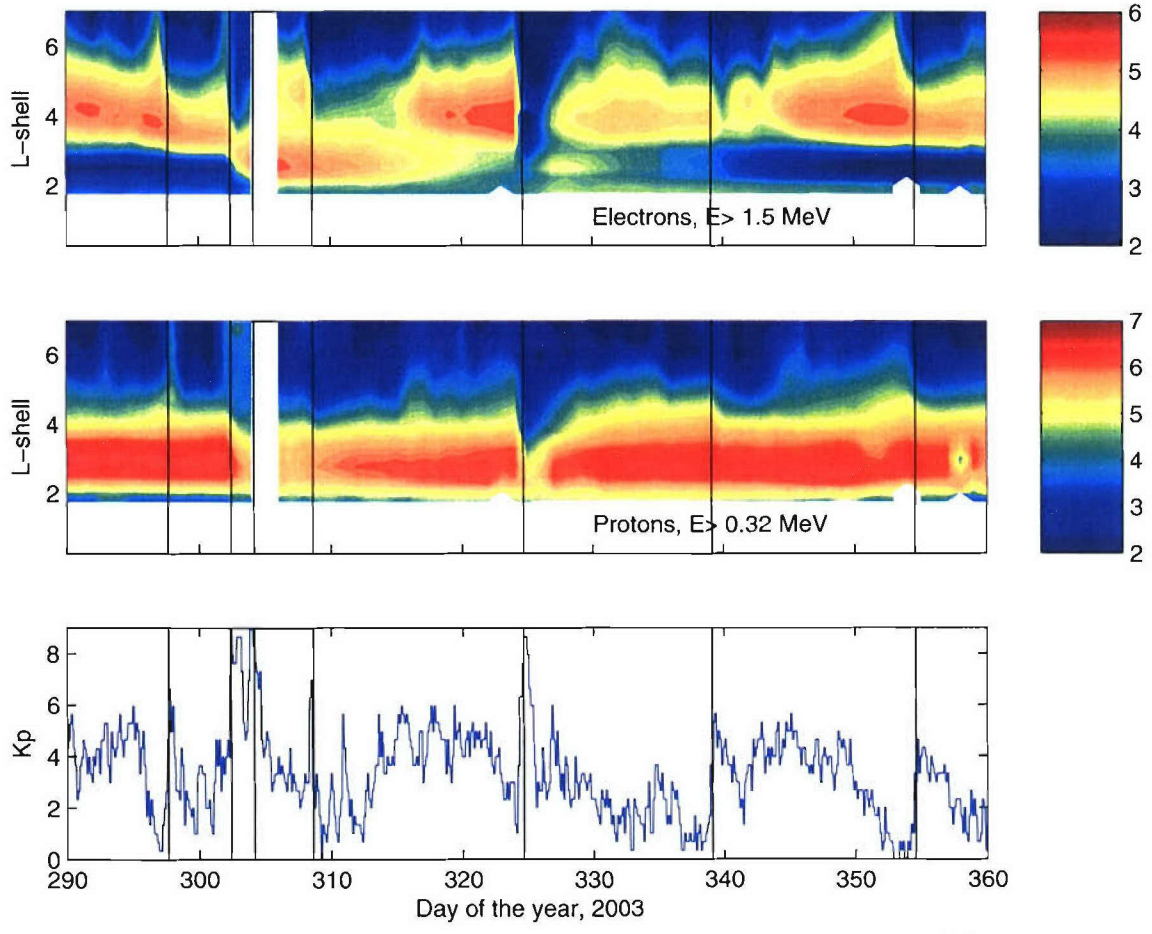

Figure 3. Integrated electron flux measured on HEO satellite Electron fluxes $E > 3.0$ MeV (top), protons $E > 0.32$ MeV (middle) in $\log_{10}(\text{cm}^{-2}\ \text{sr}^{-1}\ \text{s}^{-1})$, and *Kp* index (bottom).

4. Variable Outer Boundary Conditions

To verify whether radial diffusion is fast and efficient enough to produce radiation belt depletions down to $L = 4$, we carried out radial diffusion simulations with variable outer boundary at $L^* = 7$, which we present in Section 6. In this section, we describe the variable outer boundary used for the simulations. Geosynchronous fluxes are highly affected by adiabatic changes, producing variations by as much as 3 orders of magnitude. These adiabatic changes can be filtered out by evaluating the phase space density as a function of the third adiabatic invariant, or equivalently the L^* parameter [*Roederer, 1970*]. Once phase space density is prescribed as a function of L^*, all remaining flux variations must be caused by non-adiabatic loss or source processes. In the current study, we evaluate fluxes at $L^* = 6$ and use this to prescribe an outer boundary condition for a radial diffusion model that accounts for the non-adiabatic changes and ignores local acceleration.

Figure 4 (top panel) shows the Combined Release and Radiation Effects Satellite (CRRES) measurements of 1.0 MeV electron fluxes at $L^* = 6$, computed with T89 dynamic and OP77 static models. Since data at L^*=7 is sparse, following *Brautigam and Albert* [*2000*], we use the normalized

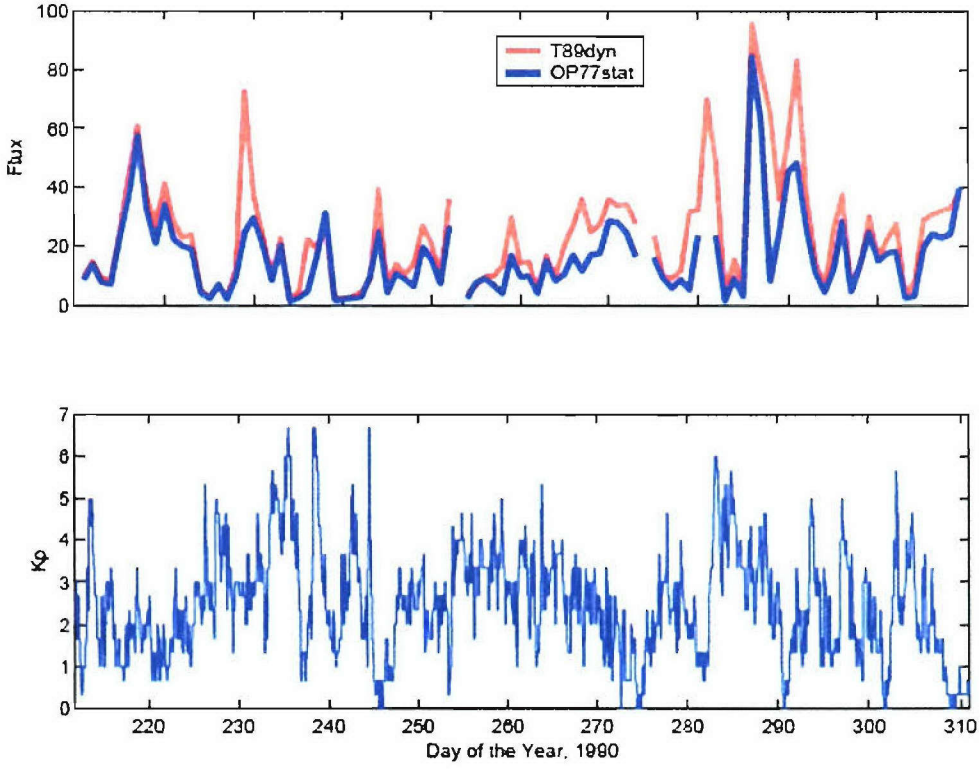

Figure 4. Daily averages of the 1-MeV electron fluxes at $L^* = 6$, measured on CRRES $\log_{10}(\text{cm}^{-2}\ \text{sr}^{-1}\ \text{s}^{-1}\ \text{keV})$,. The L^* parameter was derived using the T89 dynamic and OP77 static models.

variation at $L^* = 6$ and apply it to the average fluxes at $L^* = 7$ to produce variable boundary condition. Since radial diffusion coefficients are very high near geosynchronous orbit, phase space density tends to be flattened out by the radial diffusion [*Shprits and Thorne, 2004*]. Consequently, we can expect similar relative variation in fluxes for high L^* values. Figure 4 (bottom panel) shows the evolution of the *Kp* index. Most of the strongest electron flux depletions at $L^* = 6$ are associated with a sudden increase in *Kp*. CRRES measurements are confined to a narrow band of nearly equatorial pitch angles and will be used as a boundary condition for the radial diffusion model, which treats only 90° pitch-angle particles.

5. Model Description

Conservation of the first and second adiabatic invariants results in acceleration of particles during the inward transport and deceleration during the outward transport. The direction of the net diffusive flux is opposite to the radial gradient in phase space density. The net diffusive flux depends on the diffusion coefficients and the gradient in phase space density. If local acceleration is ignored, the temporal evolution of phase space density can be obtained from *Schulz and Lanzerotti* [*1974*]:

$$\frac{\partial f}{\partial t} = L^2 \frac{\partial}{\partial L}\left[D_{LL} L^{-2} \frac{\partial f}{\partial L}\right] - \frac{f}{\tau}, \tag{1}$$

where τ is the electron lifetime, and D_{LL} is the radial diffusion coefficient. In this formulation, the first two adiabatic invariants, *mu*μ and J*J*, are held constant and Eq. (1) can be solved numerically for *f(L,t)*. In the present study, we adopt an empirical relationship for the rate of radial diffusion due to magnetic fluctuations [*Brautigam and Albert, 2000*], which tends to dominate throughout the outer radiation zone:

$$D_{LL}^{M}(Kp, L) = 10^{(0.506Kp - 9.325)} L^{10}, Kp = 1 \text{ to } 6 \tag{2}$$

Solutions of the time-dependent code, ignoring the effects of local acceleration and only considering radial diffusion with losses, are compared to CRRES MEA observations.

The inner boundary for our simulation f(L = 1) = 0 is taken to represent loss to the atmosphere. Constant outer boundary conditions are based on averaged fluxes at L = 7 obtained from CRRES and Polar measurements (N. Meredith, P. O'Brien, personal communication). We model fluxes by an exponential fit J = 8222.6exp(–7.068K), T = 8222.6exp(–7.068K) cm–2 sr–1 keV–1 s–1, where K is kinetic energy in MeV. Variable outer boundary conditions were described in Section 3.

For simplicity, we first assume that the diffusion coefficients and lifetimes are independent of energy and solve (1) for *f(L,t)*, normalized to unity at the outer boundary. This solution will be the same for all μ values. Consequently, to obtained *f(E, L)*, the normalized phase space density should be multiplied by $J(E^*)/p^{*2}$, where E^* and p^* are the kinetic energy and momentum of the particles adiabatically scaled to the outer boundary, and J is a differential flux at the outer boundary. *Shprits et al.* [2005a] showed that for simulations with constant outer boundary conditions, parameterizations of lifetimes $\tau = 3/Kp$ is optimum for reproducing observations. Since maximum radial diffusion rates during storms correlate with depletions of the outer zone fluxes, introduction of the variable boundary results in a lower net diffusive flux. For simulations with variable outer boundary, lifetime parameterizations $\tau = 5/Kp$ produced best agreement with CRRES observations in terms of the location of the peak of fluxes and the radial extent of fluxes. Since chorus scattering rates do not show significant L dependence [*Thorne et al.*, 2005b], we adopt a lifetime parameter independent of L.

6. Simulations with Variable and Constant Outer Boundary.

To verify that outward radial diffusion, driven by losses at magnetopause and outer boundary variations around geosynchronous orbit, can produce significant depletions in the heart of the radiation belts, we conducted numerical simulations with both variable and constant outer boundary conditions, as described in Section 4. We chose a modeling period from July 19, 1990 (DOY 210) until November, 6, 1990 (DOY 310) and compared results of the radial diffusion simulation to CRRES measurements at 1 MeV. During this time, *Kp* was less than 6 for which diffusion coefficients (2) are valid. Figure 5 (top panel) shows radial diffusion simulations with constant outer boundary conditions. Our radial diffusion model predicts almost instantaneous increases in the 1-MeV fluxes during the main phase of the storm when diffusion coefficients maximize. In contrast, CRRES observations (second panel) show depletions during the main phase of the storms. Results of the simulations with variable outer boundary (bottom panel) are in better agreement with observations at high L-shells. Enhanced radial diffusion down to $L = 4$ causes fluxes to respond rapidly to outer boundary varia

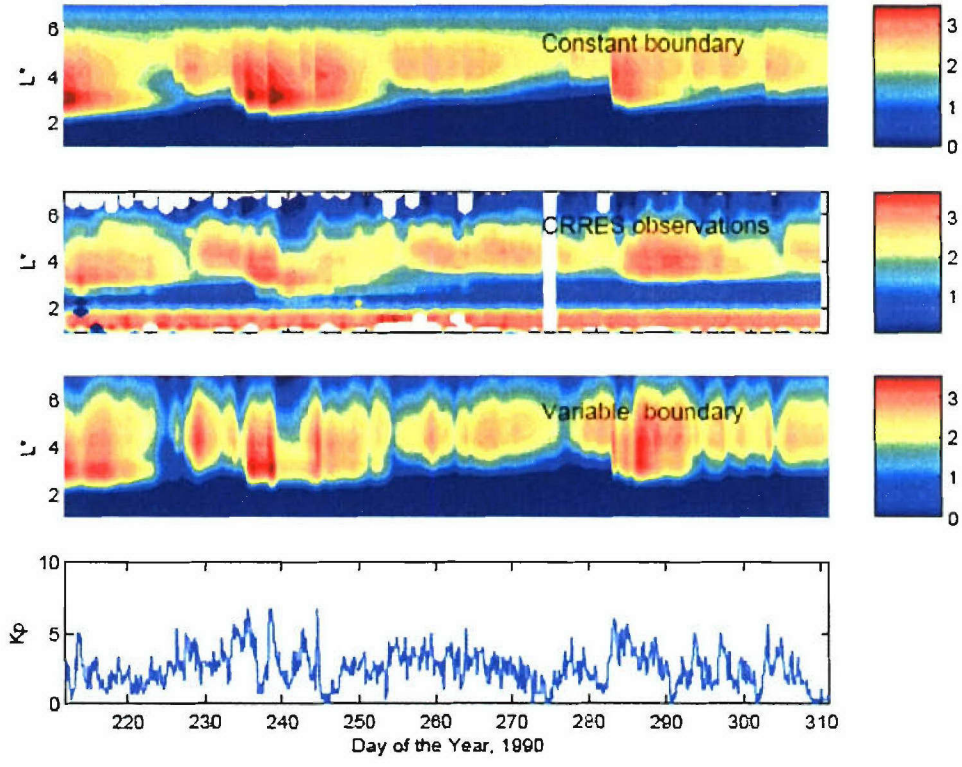

Figure 5. 1-MeV electron fluxes computed with the radial diffusion code and constant outer boundary (top panel). CRRES MEA observations of 1-MeV electron fluxes (second panel). Radial diffusion simulations with variable outer boundary (third panel). Differential flux is color-coded in $\log_{10}(\text{cm}^{-2}\ \text{sr}^{-1}\ \text{s}^{-1}\ \text{keV}^{-1})$. Evolution of the *Kp* index. Time interval from July 19, 1990 (DOY 210) till November, 6, 1990 (DOY 310).

tions. We conclude that magnetopause losses together with outward radial diffusion are capable of explaining the main phase depletions in the radiation belts down to $L = 4$. The differences between model results and observations may be due to the neglect of EMIC wave scattering, which provides additional losses at lower L, and the neglect of the chorus wave scattering, which may locally accelerate electrons.

Figure 6 shows a comparison of the two models for one of the strongest depletions of the radiation belts during the August 26, 1990 storm (DOY 238). Solar wind density, as observed on IMP8 satellite, reached 40 cc^{-1}, while solar wind speed was above 700 ms^{-1}. Such dramatic increases in the solar wind dynamic pressure compressed the magnetopause to low L-values and produced significant losses near the geosynchronous orbit. This decrease in the outer boundary flux was propagated to a lower L-shell by the outward radial diffusion. Radial diffusion even overestimates losses during this time period, possibly due to the neglect of any local acceleration processes that operate in the recovery phase of many storms [*Horne et al., 2005*].

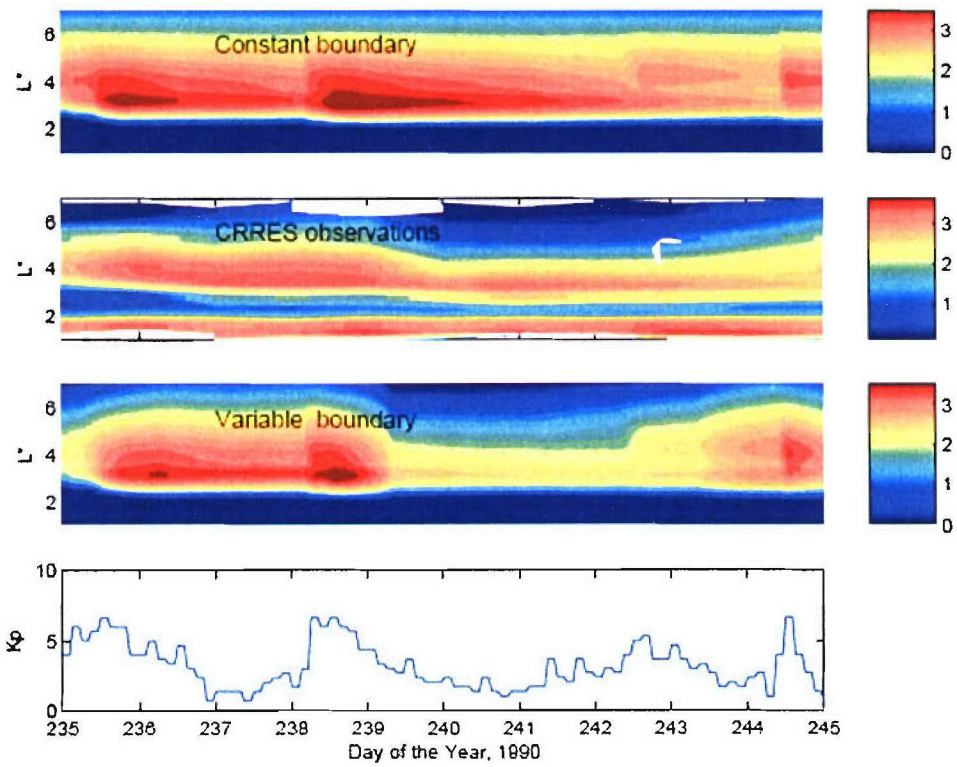

Figure 6. Same as Figure 5 but for August 23 till September 2, 1990

7. Summary and Discussion

The HEO, SAMPEX, and CRRES observations presented above indicate that main phase depletions are correlated with increases in the solar wind dynamic pressure and increases in geomagnetic activity. They occur at energies from a few hundred keV to a few MeV. EMIC wave scattering could provide very fast losses on the scale of hours and may be responsible for MeV electron loss in the heart of the radiation belt but can not explain the radiation belt depletions at higher L-shells, which occur down to a few hundred keV.

Comparison between the radial diffusion simulations and CRRES MEA observations indicate that radial diffusion is fast and efficient enough to propagate outer boundary variations down to $L = 45$. Scattering loss due to EMIC waves may also play an important role at lower L-values and compete with local acceleration, which will be most efficient just outside the plasmasphere. The results of our simulations indicate that radial diffusion can effectively redistribute outer radiation belt fluxes and smooth PSD gradients that are produced by losses to magnetopause and convection of plasma sheet electrons or by local acceleration and loss. While our results clearly show that radial diffusion is important in transporting relativistic electrons across the L-shells, it still remains unclear whether a majority of the relativistic electrons in the radiation belts came from the plasma sheet and were transported inwards or were accelerated inside the radiation belts and than diffused out.

7. Summary and Discussion

The HEO, SAMPEX, and CRRES observations presented above indicate that main phase depletions are correlated with increases in the solar wind dynamic pressure and increases in geomagnetic activity. They occur at energies from a few hundred keV to a few MeV. EMIC wave scattering could provide very fast losses on the scale of hours and may be responsible for MeV electron loss in the heart of the radiation belt but can not explain the radiation belt depletions at higher L-shells, which occur down to a few hundred keV.

Comparison between the radial diffusion simulations and CRRES MEA observations indicate that radial diffusion is fast and efficient enough to propagate outer boundary variations down to $L = 45$. Scattering loss due to EMIC waves may also play an important role at lower L-values and compete with local acceleration, which will be most efficient just outside the plasmasphere. The results of our simulations indicate that radial diffusion can effectively redistribute outer radiation belt fluxes and smooth PSD gradients that are produced by losses to magnetopause and convection of plasma sheet electrons or by local acceleration and loss. While our results clearly show that radial diffusion is important in transporting relativistic electrons across the L-shells, it still remains unclear whether a majority of the relativistic electrons in the radiation belts came from the plasma sheet and were transported inwards or were accelerated inside the radiation belts and than diffused out.

References

Abel, B., and R. M. Thorne (1998), Electron scattering loss in Earth's inner magnetosphere, 1, Dominant physical processes, *J. Geophys. Res.*, **103**, 2385

Albert, J. M., (1994),. Quasi-linear pitch angle diffusion coefficients: Retaining high harmonics, *J. Geophys. Res.*, **99**(A12), 23741–23746, 10.1029/94JA02345,

Albert, J. M. (2003), Evaluation of quasi-linear diffusion coefficients for EMIC waves in a multispecies plasma, *J. Geophys. Res.*, **108**, (A6), 1249, doi:10.1029/2002JA009792

Albert, J. M.(2005), Evaluation of quasi-linear diffusion coefficients for whistler mode waves in a plasma with arbitrary density ratio, *J. Geophys. Res.*, **110**, A03218, doi:10.1029/2004JA010844

Baker D. N., S. G. Kanekal, X. Li, S. P. Monk, J. Goldstein, and J. L. Burch (2004), An extreme distortion of the Van Allen belt arising from the Halloween solar storm in 2003, *Nature,* 878–880

Brautigam, D. H. and Albert J. M. (2000), Radial diffusion analysis of outer radiation belt electrons during the October 9, 1990 magnetic storm, *J. Geophys. Res.*, **105** (A1), 291

Elkington, S. R., M. K. Hudson, A. A. Chan (2003), Resonant acceleration and diffusion of outer zone electrons in a n asymmetric geomagnetic field, *J. Geophys. Res.*, **108** (A3),1116, doi:10.1029/2001JA009202

Green, J. C., and M. G. Kivelson (2004), Relativistic electrons in the outer radiation belt: Differentiating between acceleration mechanisms, *J. Geophys. Res.*, **109**, A03213, doi:10.1029/2003JA010153.

Green J. C., T. G. Onsager, T. P. O'Brien, and D. N. Baker (2004), Testing loss mechanisms capable of rapidly depleting relativistic electron flux in the Earth's outer radiation belt, *J. Geophys. Res.*, **109** A12211, doi:10.1029/2004JA010579.

Horne, R. B., and R. M. Thorne (1993), On the preferred source location for the convective amplification of ion cyclotron waves, *J. Geophys. Res.*, **98**(A6), 9233–9248, 10.1029/92JA02972.

Horne R. B., R. M. Thorne, S. A. Glauert, J. M. Albert., N. P. Meredith., and R. R, Anderson (2005), Timescales for radiation belt electron acceleration by whistler mode chorus, *J. Geophys. Res*, **110**, A03225, doi:10.1029/2004JA010811.

Jordanova, V. K., C. J. Farrugia, R. M. Thorne, G. V. Khazanov, G. D. Reeves, and M. F. Thomsen (2001a), Modeling ring current proton precipitation by electromagnetic ion cyclotron waves during the May 14–16, 1997, storm, *J. Geophys. Res.*, **106**(A1), 7-22, 10.1029/2000JA002008.

Jordanova, V. K., R. M. Thorne, C. J. Farrugia, Y. Dotan, J. F. Fennell, M. F. Thomsen, G. D. Reeves, and D. J. McComas (2001b), Ring current dynamics during the July 13-18, 2000 storm period, *Solar Phys.*, **204**, 361–375.

Kozyra, J. U., et al., Modeling of the contribution of electromagnetic ion cyclotron (EMIC) waves to stormtime ring current erosion, in *Magnetic Storms. Geophys. Monogr. Ser.*, vol. 98, edited by B. T. Tsurutani, et al., p. 187, AGU, Washington, D. C., 1997.

Kim, H. J. and A. A. Chan (1997), Fully-adiabatic changes in storm-time relativistic electron fluxes. *J. Geophys. Res.*, **102**:22107–22116,

Li, X., D. N. Baker, M. Temerin, T. E. Cayton, E. G. D. Reeves, R. A. Christensen, J. B. Blake, M. D. Looper, R. Nakamura, and S. G. Kanekal (1997), Multisatellite observations of the outer zone electron variation during the November 3 - 4, 1993, magnetic storm, *J. Geophys. Res.*, **102**(A7), 14123-14140, 10.1029/97JA01101.

Li, X., I. Roth, M. Temerin, J. R. Wygant, M. K. Hudson, and J. B. Blake (1993), Simulation of the prompt energization and transport of radiation belt particles during the March 24, 1991 SSC, *Geophys. Res. Lett.*, **20***(22)*, 2423-2426, 10.1029/93GL02701

Lopez, R. E. , Baker, D. N. and Allen, J. H. (2004), Sun unleashes Halloween storm, *Eos*, **85**, 105-108

Lyons, L. R., R. M. Thorne, and C. F. Kennel (1972), Pitch angle diffusion of radiation belt electrons within the plasmasphere, *J. Geophys. Res.*, 77, 3455.

Lyons, R. L. and R. M. Thorne (1973), Equilibrium structure of radiation belt electrons, *J. Geophys. Res.*, **77**, 3455

Mathie, R. A., and I. R. Mann, A correlation between extended intervals of ULF wave power and storm-time geosynchronous relativistic electron flux enhancements, *Geophys. Res. Lett.*, **27**, 3261, 2000.

McAdams, K. L., G. D. Reeves (2001), Non-adiabatic response of relativistic radiation belt electrons to GEM magnetic storms, *Geophys. Res. Lett.*, **28**(9), 1879-1882, 10.1029/2000GL011998,

Meredith N. P., R. M. Thorne, R. B. Horne, D. Summers, B. J. Fraser, R. R. Anderson (2003), Statistical analysis of relativistic electron energies for cyclotron resonance with EMIC waves observed on CRRES, *J. Geophys. Res.*, **108** (A6), 1250, doi:10.1029/2002JA009700

Meredith, M. P., R. B. Horne, R. M. Thorne, D. Summers, and R. R. Anderson, Substorm dependence of plasmaspheric hiss, *J. Geophys. Res.*, **109**, A06209, doi:10.1029/2004JA010387, 2004.

Millan, R. M., et al., X-ray observations of MeV electron precipitation with a balloon-borne germanium spectrometer, *Geophys. Res. Lett.*, *29*(24), 2194, doi:10.1029/2002GL015922, 2002.

Nagai, T., 'Space weather forecast": Prediction of relativistic electron intensity at synchronous orbit, *Geophys. Res. Lett.*, **15**(5), 425-428, 10.1029/88GL02094, 1988.

O'Brien, T. P. , McPherron, R. L. , Sornette, D. , Reeves, G. D. , Friedel, R. , Singer, H. J. (2001) Which magnetic storms produce relativistic electrons at geosynchronous orbit? *J. Geophys. Res.* **106** , No. A8 , p. 15,533 (2001JA000052).

O'Brien, T. P., M. D. Looper , and J. B. Blake (2004), Quantification of relativistic electron Micro-bursts losses during the GEM storms, *Geophys. Res. Lett.*, **31**, L04802, doi:10.1029/2003GL018621

Onsager T. G., G. Rostoker, H.-J. Kim, G. D. Reeves, T. Obara, H. J. Singer, and C. Smithtro, Radiation belt electron flux dropouts: Local time, radial, and particle-energy dependence, *J. Geophys. Res.*, **107** (A11), 1382, doi:10.1029/2001JA000187, 2002.

Reeves, G. D., D. N. Baker, R. D. Belian, J. B. Blake, R. E. Cayton, J. F. Fennell, R. H. W. Friedel, M. M. Meier, R. S. Selesnick, and H. E. Spence, (1998) The global response of relativistic radiation belt electrons to the January 1997 magnetic cloud, *Geophys. Res. Lett.*, **25**, 3265-3268

Reeves G. D., K. L. McAdams, R. H. W. Friedel, T. P. O'Brien, Acceleration and loss of relativistic electrons during geomagnetic storms, (2003) *Geophys. Res. Lett.*, **30** *(10)*, 1529, doi:10.1029/2002GL016513,

Roederer, J. G., *Dynamics of Geomagnetically Trapped Radiation*, Springer-Verlag, New York, 1970.

Russell C. T. and Thorne, R. M. (1970) On the structure of the inner magnetosphere, Cosmic Electrodynamics,

Schulz, M., and L. J. Lanzerotti, Particle Diffusion in the Radiation Belts (1974)., vol. 7 of Physics and Chemistry in Space, Springer-Verlag, New York,

Shprits Y. Y. and Thorne, R. M, (2005), Time dependent radial diffusion modeling of relativistic electrons with realistic loss rate, *Geophys. Res., Lett.*, **31**, doi:10.1029/2002JA009791,

Shprits, Y. Y., R. M. Thorne, G. D. Reeves, and R. Friedel, (2005a) Radial diffusion modeling with empirical lifetimes: Comparison with CRRES observations, *Annales Geophys.* **23,** 1467-1471

Shprits, Y. Y,. R. M. Thorne, R. B. Horne, S. A. Glauert, M. Cartwright, C. T. Russell, D. N. Baker and S. G. Kanekal, (2005b) Acceleration mechanism responsible for the formation of the new radiation belt during the 2003 Halloween Solar storm, *Geophys. Res., Lett.* submitted.

Shue, J.-H., J. K. Chao, H. C. Fu, C. T. Russell, P. Song, K. K. Khurana, H. J. Singer (1997), A new functional form to study the solar wind control of the magnetopause size and shape, *J. Geophys. Res.*, **102**(A5), 9497-9512, 10.1029/97JA00196,

Summers D, and R. M. Thorne, (2003), Relativistic electron pitch-angle scattering by electromagnetic ion cyclotron waves during geomagnetic storms, *J. Geophys. Res.*, **108**, (A4), 1143, doi:10.1029/2002JA009489.

Thorne R. M. and C. F. Kennel (1971),. Relativistic electron precipitation during magnetic storm main phase, *J. Geophys. Res.*, **76**, 4446.

Thorne R. M., Horne, S. Glauert, N. Meredith, Y. Y. Shprits, D. Summers, and R. Anderson (2005a), The Influence of Wave-Particle Interactions on Relativistic Electron Dynamics During Storms, in Inner Magnetosphere Interaction: New Perspectives from Imaging, *Geophys. Monogr. Ser.*, vol 159, edited by J. Burch, M. Schulz and H. Spence, AGU, Washington D. C.

Thorne R. M., T. P. O'Brien, Y. Y. Shprits, D. Summers, and R. B. Horne (2005b), Timescale for MeV electron microburst loss during storms, *J. Geophys. Res.*, **110**, A09202, doi:10.1029/2004JA010882.

LABORATORY OPERATIONS

The Aerospace Corporation functions as an "architect-engineer" for national security programs, specializing in advanced military space systems. The Corporation's Laboratory Operations supports the effective and timely development and operation of national security systems through scientific research and the application of advanced technology. Vital to the success of the Corporation is the technical staff's wide-ranging expertise and its ability to stay abreast of new technological developments and program support issues associated with rapidly evolving space systems. Contributing capabilities are provided by these individual organizations:

Electronics and Photonics Laboratory: Microelectronics, VLSI reliability, failure analysis, solid-state device physics, compound semiconductors, radiation effects, infrared and CCD detector devices, data storage and display technologies; lasers and electro-optics, solid-state laser design, micro-optics, optical communications, and fiber-optic sensors; atomic frequency standards, applied laser spectroscopy, laser chemistry, atmospheric propagation and beam control, LIDAR/LADAR remote sensing; solar cell and array testing and evaluation, battery electrochemistry, battery testing and evaluation.

Space Materials Laboratory: Evaluation and characterizations of new materials and processing techniques: metals, alloys, ceramics, polymers, thin films, and composites; development of advanced deposition processes; nondestructive evaluation, component failure analysis and reliability; structural mechanics, fracture mechanics, and stress corrosion; analysis and evaluation of materials at cryogenic and elevated temperatures; launch vehicle fluid mechanics, heat transfer and flight dynamics; aerothermodynamics; chemical and electric propulsion; environmental chemistry; combustion processes; space environment effects on materials, hardening and vulnerability assessment; contamination, thermal and structural control; lubrication and surface phenomena. Microelectromechanical systems (MEMS) for space applications; laser micromachining; laser-surface physical and chemical interactions; micropropulsion; micro- and nanosatellite mission analysis; intelligent microinstruments for monitoring space and launch system environments.

Space Science Applications Laboratory: Magnetospheric, auroral and cosmic-ray physics, wave-particle interactions, magnetospheric plasma waves; atmospheric and ionospheric physics, density and composition of the upper atmosphere, remote sensing using atmospheric radiation; solar physics, infrared astronomy, infrared signature analysis; infrared surveillance, imaging and remote sensing; multispectral and hyperspectral sensor development; data analysis and algorithm development; applications of multispectral and hyperspectral imagery to defense, civil space, commercial, and environmental missions; effects of solar activity, magnetic storms and nuclear explosions on the Earth's atmosphere, ionosphere and magnetosphere; effects of electromagnetic and particulate radiations on space systems; space instrumentation, design, fabrication and test; environmental chemistry, trace detection; atmospheric chemical reactions, atmospheric optics, light scattering, state-specific chemical reactions, and radiative signatures of missile plumes.

THE AEROSPACE CORPORATION
2350 E. El Segundo Boulevard
El Segundo, California 90245-4691
U.S.A.